



PLASTICITY OF CEREBRAL METABOLIC WHISKER MAPS IN ADULT MICE AFTER WHISKER FOLLICLE REMOVAL— II. MODIFICATIONS IN THE SUBCORTICAL SOMATOSENSORY SYSTEM

P. MELZER* and C. B. SMITH†

Laboratory of Cerebral Metabolism, National Institute of Mental Health, Building 36, Room 1A05,
 36 Convent Drive MSC 4030, Bethesda, MD 20892-4030, U.S.A.

Abstract—The follicles of whiskers C1–3 were removed from the left side of the snout of adult mice. Adjacent whiskers B1–3 and D1–3 were stimulated while local rates of glucose utilization were measured with the [¹⁴C]2-deoxyglucose method two, four, eight, 64, 160 and ~250 days after follicle removal. Local metabolic activity in the trigeminal sensory brainstem and somatosensory thalamus was compared with that of unoperated mice with the same stimulation and of mice with the same lesion that had all whiskers clipped. Actual rates of glucose utilization were measured in brainstem subnuclei caudalis and interpolaris whereas metabolic activation was only assessable by colour-coded imaging in brainstem nucleus principalis and in the thalamic ventrobasal complex.

Whisker stimulation activated the somatotopically appropriate loci in brainstem and thalamus. In addition, the territory deprived by follicle removal was metabolically activated in subnuclei caudalis and interpolaris at all time intervals examined. The activation was statistically significant in subnucleus interpolaris at two days, indicating that the metabolic representations of whiskers neighbouring the lesion rapidly expanded into the deprived territory. Nucleus principalis showed a broad metabolic activation at two and four days that was absent at the longer time intervals examined. Instead, at ~250 days the metabolic representations of the whiskers adjacent to the lesion were enlarged into the deprived territory as in the subnuclei. Since metabolic whisker representation in the ventrobasal complex appeared to have changed in the same fashion, follicle removal apparently resulted in congruent modifications of the whisker map in the three nuclei of termination as well as in the thalamic relay at the longest time interval examined. Since metabolic responsiveness of the deprived barrels in barrel cortex of the same animals increased statistically significantly only several months after follicle removal, the novel neural responses in the brainstem were not effectively transmitted to barrel cortex immediately and the slowly evolving cortical modifications are more likely to be associated with regrowth of the connectivity of primary neurons.²⁸ By contrast, unmasking of hitherto suppressed inputs may underlie the early expansion of metabolic whisker representation in the brainstem. © 1997 IBRO. Published by Elsevier Science Ltd.

Key words: vibrissa, trigeminal brainstem, ventrobasal complex, deoxyglucose.

The present study constitutes the second part of our investigation on the effects of the removal of the follicles of whiskers C1–3 on whisker maps in the whisker-to-barrel pathway of adult mice. While the companion report focuses on plasticity of somatotopic representation in barrel cortex and its relationship to the regeneration of peripheral innervation, the present report describes the modifications of whisker representations in subcortical relay stations of the pathway. The whiskers on the snout are represented somatotopically by cytochrome oxidase- and succinic

dehydrogenase-rich cytoarchitectonic segments in brainstem subnucleus caudalis, subnucleus interpolaris and nucleus principalis as well as in the thalamic ventrobasal complex.^{5,6,12,27,40,44} In the present study, the segments were used as landmarks to detect changes in metabolic activation after whisker follicle removal with the autoradiographic deoxyglucose method.³⁸ Local cerebral metabolic rates for glucose (ICMR_{glc}) were measured in subnuclei caudalis and interpolaris, but could not be determined in nucleus principalis, because of the limited spatial resolution of the method, and in the ventrobasal complex, because morphological whisker representations could not be delineated satisfactorily. However, colour-coded images demonstrated noticeable changes in metabolic activation in the two stations, affirming that follicle removal affected these stations of the whisker-to-barrel pathway in a similar fashion as the subnuclei. Preliminary results of the present study have been published as an abstract.³⁰

*Present address: Department of Psychology and Institute for Developmental Neuroscience, John F. Kennedy Center for Research on Human Development, Box 152 Peabody College, Vanderbilt University, Nashville, TN 37203, U.S.A.

†To whom correspondence should be addressed.

Abbreviation: ICMR_{glc}, local cerebral metabolic rate for glucose.

EXPERIMENTAL PROCEDURES

Animals

The material for the present study was obtained from the same mice used in the companion report²⁸ where the procedures are described in greater detail. All procedures were in accordance with the National Institutes of Health Guide for the Care and Use of Laboratory Animals and were approved by the NIMH Animal Care and Use Committee. All efforts were made to minimize animal suffering, to reduce the number of animals used, and to utilize alternatives to *in vivo* techniques. Male and female Swiss albino mice of International Charles Rivers origin (Harlan Sprague Dawley, Indianapolis, IN, U.S.A.), >2 months-of-age, were used. The follicles of the left whiskers C1, C2 and C3 were surgically removed.

Measurement of rates of glucose utilization in barrel cortex

Preparation of animals. Measurements of local rates of glucose utilization were carried out in five to nine stimulated and unstimulated mice two, four, eight, 64, 160 ± 3 days and 250 ± 45 days after follicle removal and in 10 age-matched mice without follicular lesions that were subjected to the same whisker stimulation as mice with lesions. On the day prior to the deoxyglucose study, a femoral artery and vein were catheterized. Mice that were to be stimulated had wire pieces glued on left whiskers B1-3 and D1-3. All other whiskers were clipped close to the skin. Unstimulated mice with lesions had all whiskers on both sides clipped. Further details are provided in the companion report.²⁸ On the following day, 2-deoxy-D-[1-¹⁴C]glucose (DuPont-NEN, Wilmington, DE, U.S.A.; specific activity 50–55 mCi/mmol, dose 120–150 μ Ci/kg) in heparinized saline was injected intravenously, whisker stimulation with magnetic field bursts was initiated and timed arterial blood samples were collected. Arterial blood pressure, haematocrit, blood gases, blood pH and the arterial plasma glucose concentration were recorded (see companion report²⁸ for the physiological variables).

The mice were killed at a precisely recorded time 45–50 min after tracer injection. The brains were removed, divided and frozen. Alternate series of 20 μ m-thick sections were cut in a cryostat transverse through the brainstem and oblique to horizontal through the thalamus. Sections of the brainstem were obtained from all animals. Sections of the thalamus were obtained from stimulated and unstimulated mice ~250 days after follicle removal and age-matched stimulated unoperated controls. One section series was dried on a hotplate, autoradiographed together with calibrated plastic [¹⁴C]standards on X-ray film (Ektascan[®] EMC-1, Eastman Kodak Co., Rochester, NY, U.S.A.) and stained for cytochrome oxidase activity.⁴³ The other series was air-dried and stained for Nissl substance.

Densitometry. Autoradiograms were analysed with a video camera-based image analysis system (MCID.Imaging Research, St Catharines, Ontario, Canada). Local cerebral metabolic rates for glucose (ICMR_{glc}) were measured in the areas representing whiskers A1-3, B1-3, C1-3, D1-3 and E1-3 in trigeminal sensory brainstem subnucleus caudalis and subnucleus interpolaris on both sides. The five areas were outlined on digitized images based on the segmentation in sections stained for cytochrome oxidase activity. If circumferences of the segments were not fully visible on one section, one or two adjacent sections were used to complete the outlines. The outlines were superimposed on the corresponding autoradiograms and the pixel-weighted averages of the concentration of ¹⁴C in each delineated area was determined from the area's optical density and the calibration curve obtained from the plastic standards. These measurements were repeated on autoradiograms of eight to 10 consecutive sections representing a 400 μ m region along

the caudorostral axis of a given subnucleus. Each region represented the portion of the subnucleus where the morphological representations of the whiskers were most distinct. In subnucleus caudalis this region ended 320 μ m caudally from the caudal pole of subnucleus interpolaris. In subnucleus interpolaris the region started 320 μ m rostral from its caudal pole. The ICMR_{glc} were calculated from the local concentrations of ¹⁴C and the time courses of the arterial plasma specific activities with the operational equation of the deoxyglucose method.³⁸

Metabolic rates were not measured in nucleus principalis and in the thalamic ventrobasal complex, because of the small size of the cytochrome oxidase-rich segments in the former and the absence of clear segmentation in the latter. However, we were able to compare the patterns of metabolic activity in both with the help of colour-coded, digitized images of autoradiograms (IMAGE, W. Rasband, NIMH, USPHS, Bethesda, MD, U.S.A.).

Statistical analyses. In subnuclei caudalis and interpolaris of stimulated mice, the mean differences between homeotopic areas ipsi- (left side) and contralateral (right side) to both stimulation and the lesion were compared with the differences in unstimulated mice at the same time interval after the lesion as well as the differences in stimulated unoperated controls with two-tailed Dunnett's *t*-tests (SAS[®]; SAS Institute, Cary, NC, U.S.A.).

RESULTS

Subnuclei caudalis and interpolaris

Cytochrome oxidase activity. The rows of segments of high cytochrome oxidase activity that represent the five rows of large caudal whiskers on the snout were clearly distinguishable in subnucleus caudalis (Fig. 1) and subnucleus interpolaris (Fig. 2). The segments were separated by thin bands of low enzyme activity. Whereas they appeared cohesive in subnucleus caudalis, they were fractured by criss-crossing bundles of myelinated nerve fibres and, thus, more difficult to identify in subnucleus interpolaris. In subnucleus caudalis enzyme activity in the deprived segments appeared slightly lower than that of the surrounding segments at 64 days after whisker follicle removal (Fig. 1). No change was detected in subnucleus interpolaris (Fig. 2).

Metabolic activation. In unoperated controls, stimulation of whiskers B1-3 and D1-3 increased ICMR_{glc} to the highest degree in the cytochrome oxidase-rich segments representing the stimulated whiskers in subnucleus caudalis (Fig. 1CTR) and in subnucleus interpolaris (Fig. 2CTR). Neighbouring segments appeared activated at a lower level, particularly near the boundaries with representations B1-3 and D1-3. In spite of this spread, two separate areas of metabolic activation were distinct. In both subnuclei the two areas remained most prominent at all time intervals after whisker follicle removal (Fig. 1 and Fig. 2, 2^d–250^d). However, already two days after the lesion there was a major spread of metabolic activation from representations B1-3 and D1-3 into the surround and, particularly into the deprived territory, fusing the two areas of activation

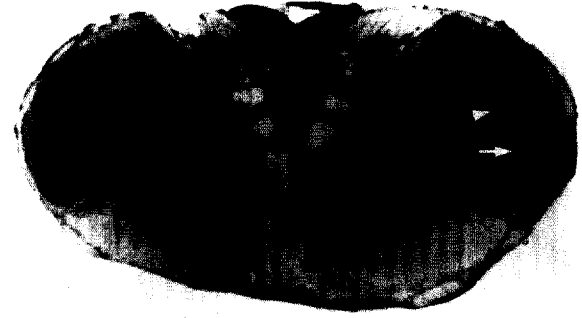
subnucleus caudalis



2d



4d



8d



64d



160d

Fig. 1. (Caption on p. 47).

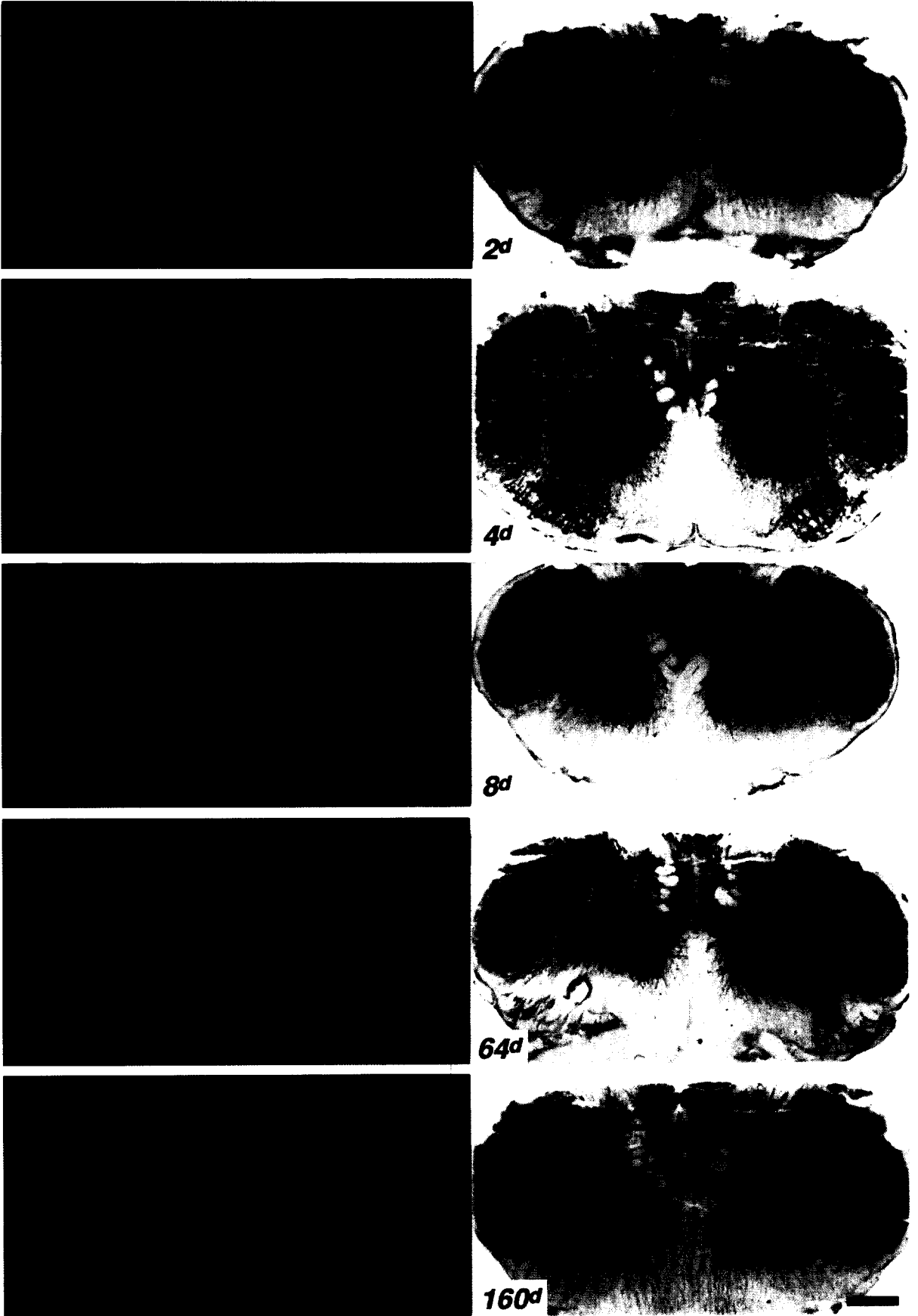


Fig. 1 (continued. Caption overleaf).

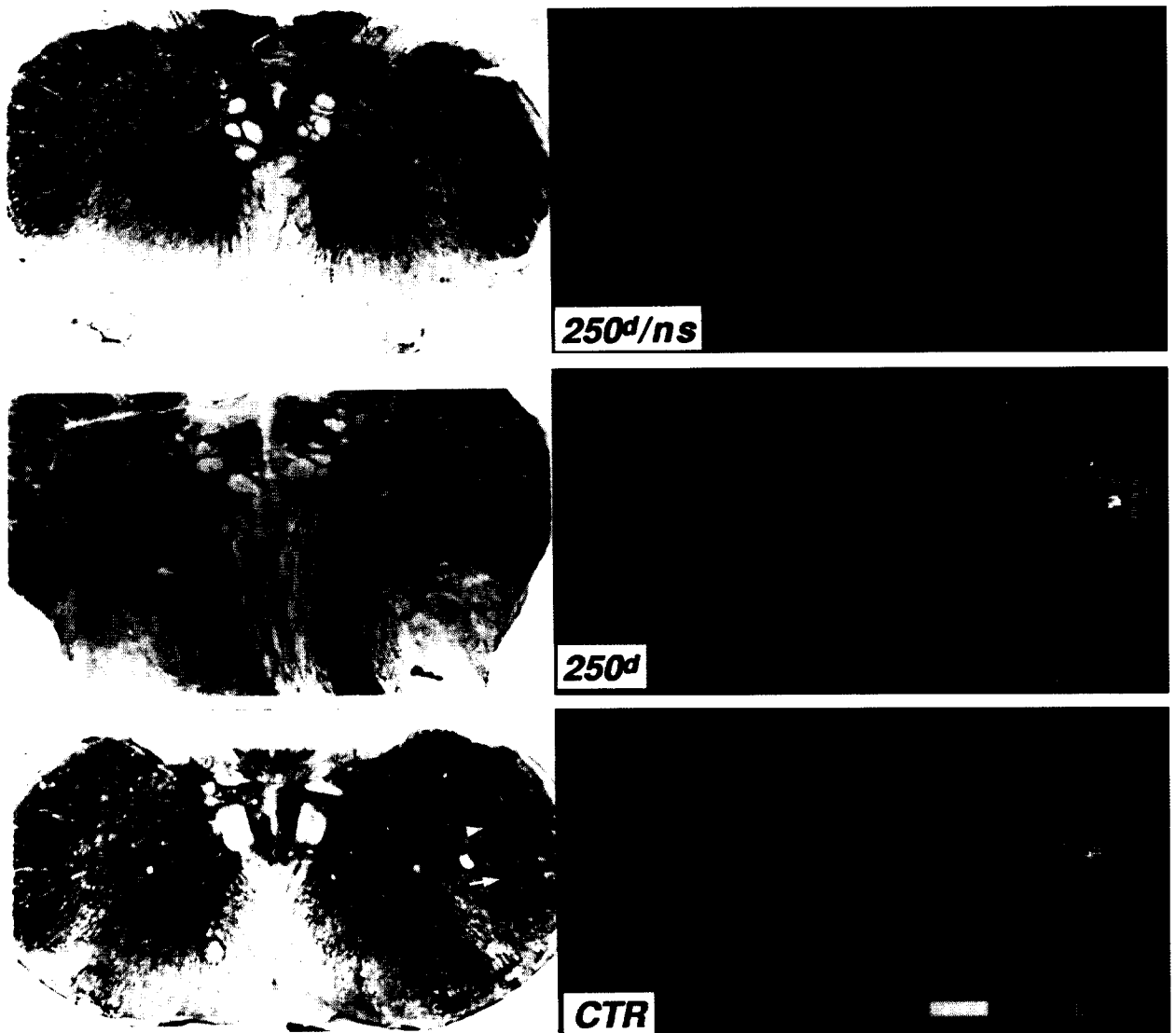


Fig. 1. Metabolic activation in subnucleus caudalis. The two facing pages display the results from mice that had the follicles of left whiskers C1, C2 and C3 surgically removed at >2 months of age and were subjected to deoxyglucose studies two (2^d), four (4^d), eight (8^d), 64 (64^d) and 160 days (160^d) after the lesion. The left page displays the results of mice that had whiskers B1–3 and D1–3 deflected during the deoxyglucose studies, the right page those of mice that had all whiskers clipped. Outer columns: Transverse sections stained for cytochrome oxidase activity after autoradiography. Inner columns: Colour-coded images of the corresponding autoradiograms. The panels on the page overleaf show the results of mice with lesions subjected to deoxyglucose studies at the longest interval after the lesion, i.e. ~250 days, with (250^d) and without whisker stimulation ($250^d/n.s.$) and of unoperated controls with the same stimulation (CTR). Left column: Transverse sections stained for cytochrome oxidase activity after autoradiography. Right column: Colour-coded images of the corresponding autoradiograms. In the cytochrome oxidase-stained sections, the five rows of enzyme-rich segments that represent whisker rows A–E are distinctive. In these rows, the caudal whiskers are represented medially. The segments representing whiskers B1 and D1 are identified by arrows and arrowheads, respectively, at eight days (8^d) and in controls (CTR). At 64 days, the segments deprived by the lesion, i.e. C1–3, stain slightly less for cytochrome oxidase activity than the adjacent segments (64^d). In the colour-coded images, the degree of metabolic activation is expressed by the colours in the bar beneath each image (white/red is high, blue is low). In the stimulated mice metabolic activation is prominent in and near the morphological representations of the deflected whiskers, i.e. ipsilateral segments B1–3 and D1–3, constituting two foci. In controls these foci are distinctly separate. In mice with lesions, there is an increase in metabolic activation of deprived segments C1–3 fusing the foci. The metabolic activity in unstimulated mice with lesions is comparably homogenous. Increased metabolic activity in the deprived territory is detectable at four days (4^d ; arrow). Contralateral metabolic activity remains low and undifferentiated (dorsal is up, the animal's left side is on the right; Scale bars at 160^d and CTR=300 μ m).

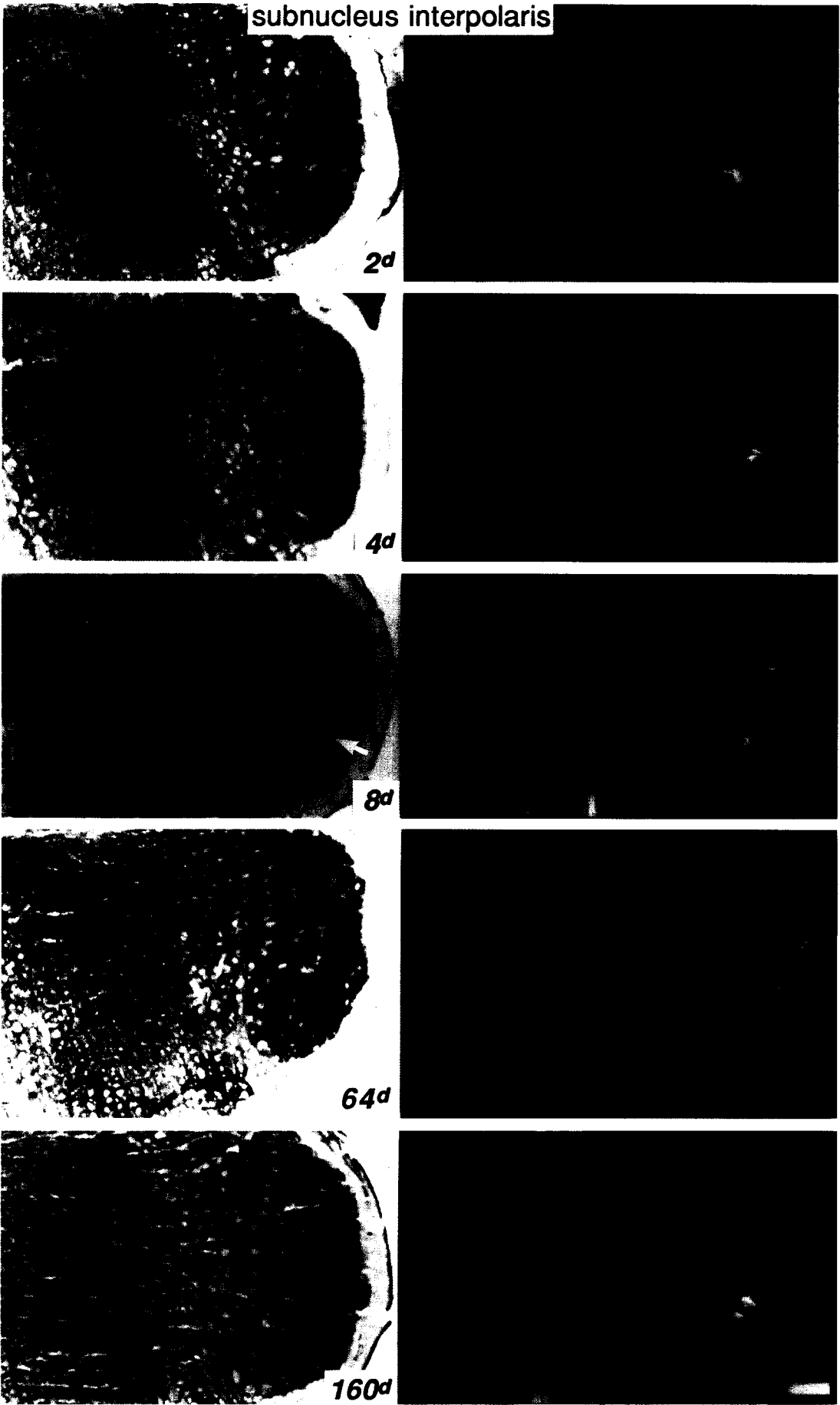


Fig. 2. (Caption on p. 50).

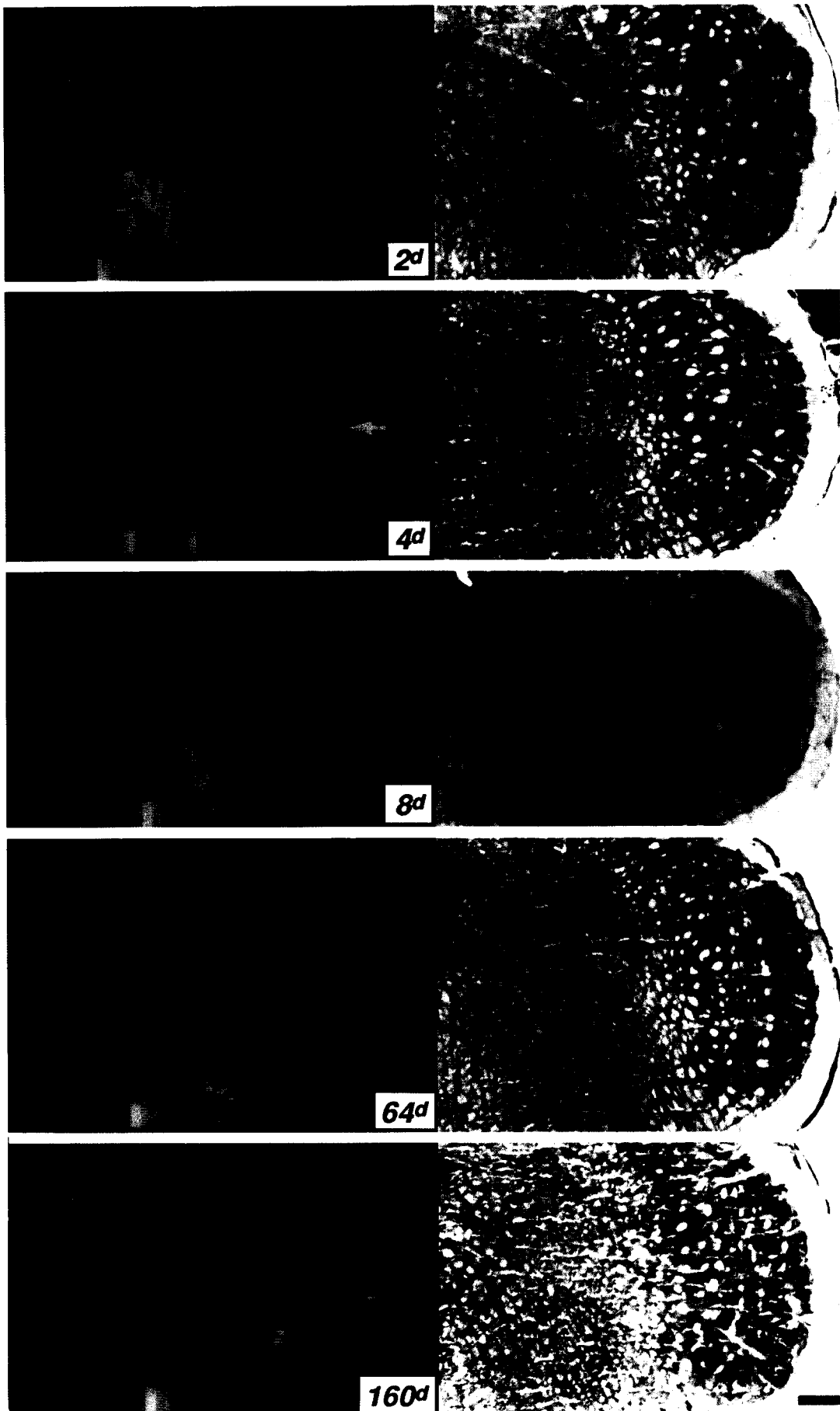


Fig. 2 (continued Caption overleaf).

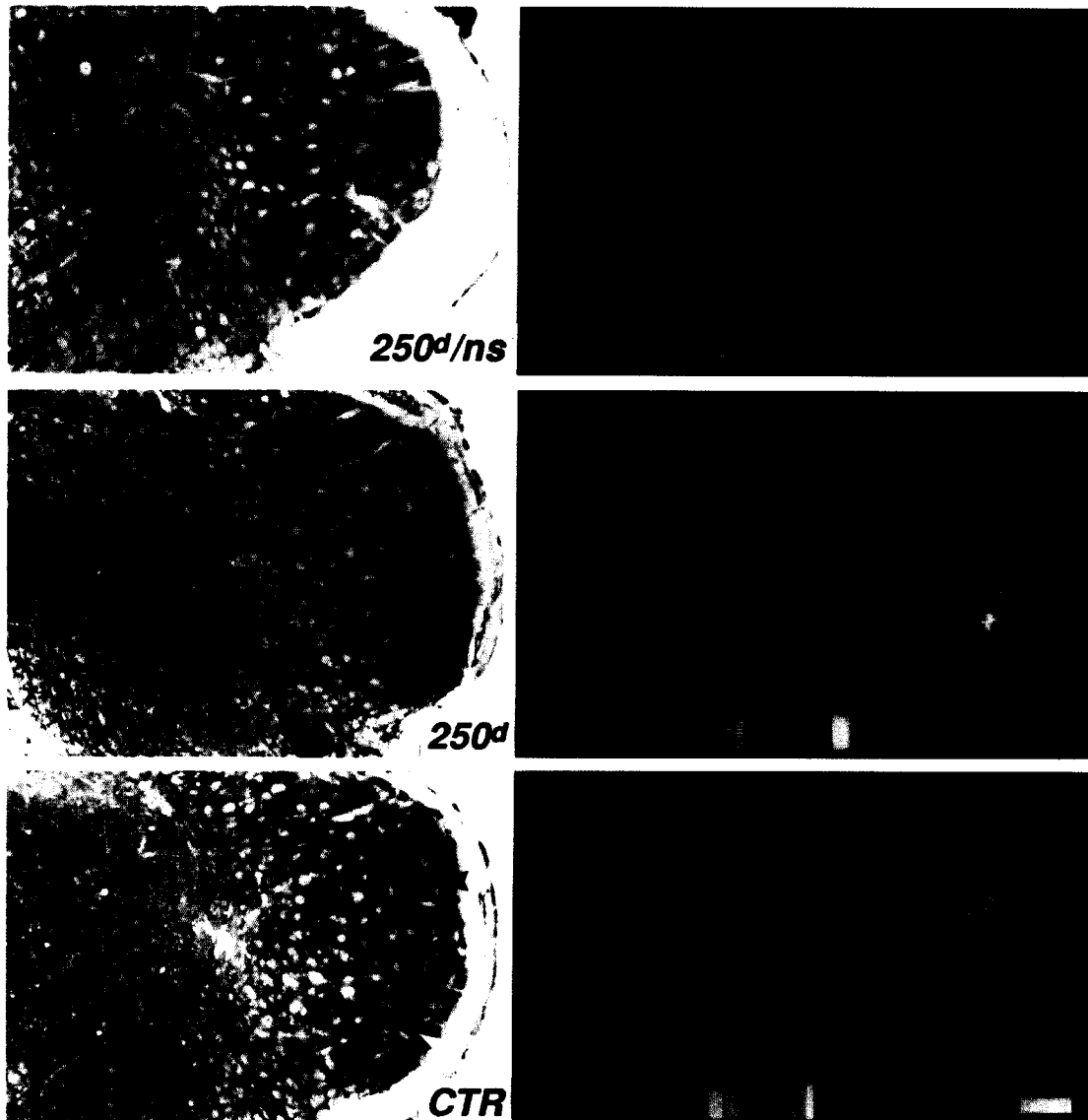


Fig. 2. Metabolic activation in subnucleus interpolaris. The results are composed as in Fig. 1, except that only the side ipsilateral to the lesion and/or stimulation is shown. In the sections stained for cytochrome oxidase activity, the five rows of enzyme-rich segments representing whisker rows A–E are distinctive. In these rows, the caudal whiskers are represented laterally. At eight days (8^d) and in the control (CTR), the segments representing whiskers B1 and D1 are identified by arrows and arrowheads, respectively. No changes in enzyme activity were detected. The colour-coded images show that the deflection of whiskers B1–3 and D1–3 increases metabolic activity prominently in the ipsilateral morphological representations of these whiskers forming two foci (white/red is high, blue is low). In the controls these foci remain distinctly separate. However, in mice with lesions metabolic activity in deprived segments C1–3 is increased fusing the two foci. In unstimulated mice with lesions, a slight increase in metabolic activity of the deprived territory is discernible on occasion (arrow at 4^d). Orientation: dorsal is up, the lateral is on the right; scale bars at 160^d and CTR=250 μ m).

(Fig. 1, $2, 2^d$). In spite of a slight waxing and waning in metabolic activity in the deprived territory of subnucleus interpolaris, the fusion of representations B1–3 and D1–3 was consolidated in both subnuclei at the longest time intervals examined (Figs 1 and 2, 160^d and 250^d). Metabolic activation was absent in unstimulated mice with lesions. In these mice, ICMR_{glc} appeared low and almost uniform at all time intervals, though an occasional small increase could

be detected in the deprived territory of both subnuclei (e.g., Figs 1, $2, 4^d$). Metabolic activity contralateral to stimulation and/or lesion remained low and undifferentiated.

The measurements of ICMR_{glc} in subnucleus caudalis (Fig. 3) and subnucleus interpolaris (Fig. 4) demonstrate that the metabolic activation (i.e. left-to-right difference in ICMR_{glc}) of representations B1–3 in both subnuclei was consistently higher than

subnucleus caudalis

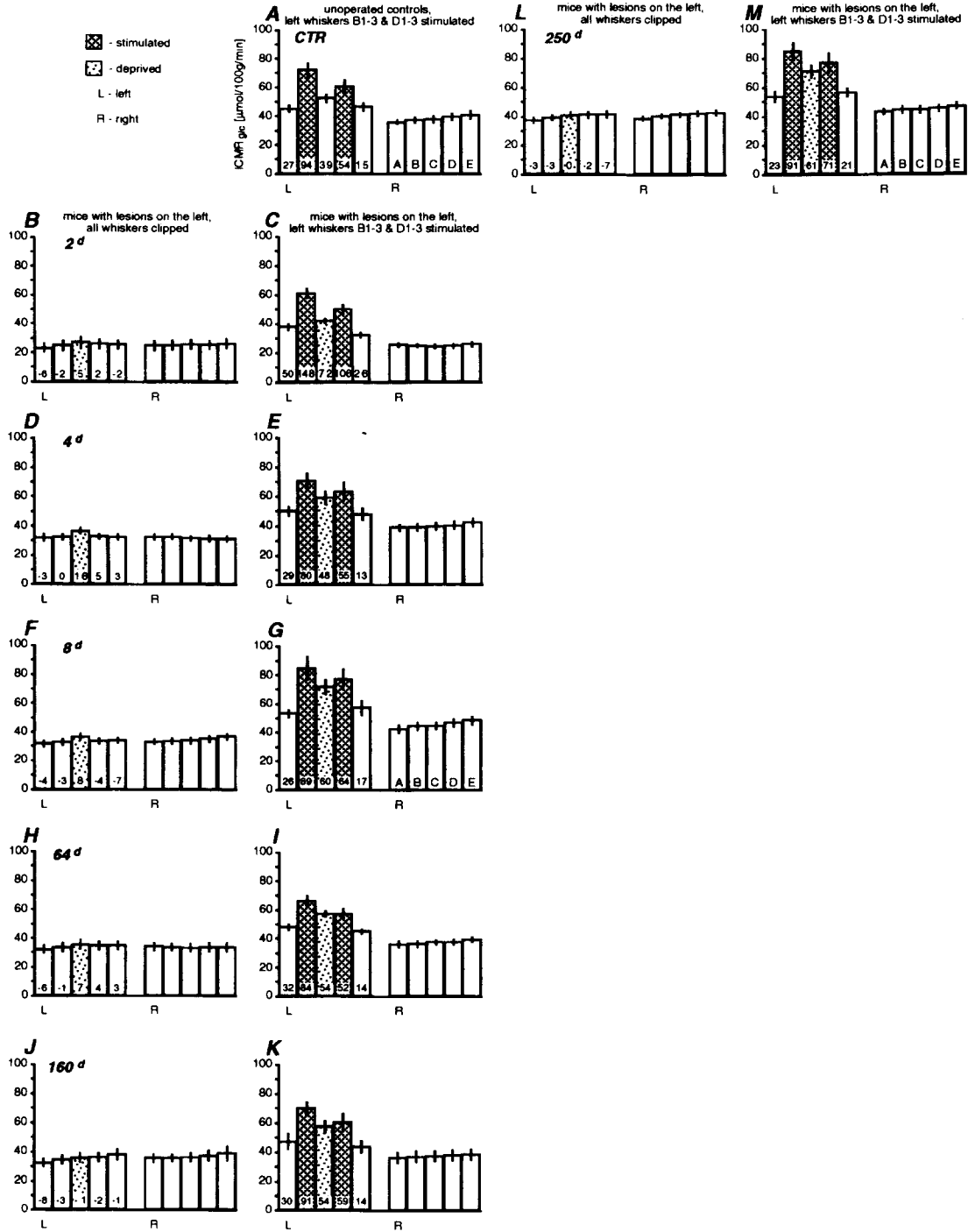


Fig. 3. Local cerebral metabolic rates for glucose ($ICMR_{glc}$) in subnucleus caudalis. The bar graphs, labelled A–M, represent the mean metabolic rates \pm S.E.M. obtained from five to ten mice for representations A1–3 (A), B1–3 (B), C1–3 (C), D1–3 (D) and E1–3 (E) ipsi- (left) and contralateral (right) to the lesion and/or stimulation. Graph A presents the data of stimulated unoperated mice (CTR). The subsequent graphs show the data obtained from mice with lesions that had all whiskers clipped before the deoxyglucose study (B, D, F, H, J and L) or had left whiskers B1–3 and D1–3 deflected during that study (C, E, G, I, K and M). The graphs are sorted by increasing time between the lesion and the deoxyglucose study. The left-to-right percent differences in metabolic rate are inserted in the bars. In stimulated unoperated mice, the highest metabolic rates were found in the morphological representations of the stimulated whiskers (A). Metabolic rates in inappropriate representations A1–3, C1–3 and E1–3 were also elevated, but to a substantially lower degree. Stimulated mice with lesions showed similar increases in metabolic rate in the appropriate representations (C, E, G, I, K and M). The metabolic rate of representations B1–3 was consistently higher than that of representations D1–3. Though there was a distinct depression in metabolic activity two days after the lesion (B and C), whisker stimulation increased metabolic rates almost to control levels (C). Beginning at four days after the lesion, the metabolic rate in deprived representations C1–3 was persistently increased above control (E, G, I, K and M) with a peak at eight days (G). In unstimulated mice with lesions the metabolic rate of the deprived territory was slightly higher than that of the adjacent areas between two and eight days after the lesion (B, D, and F).

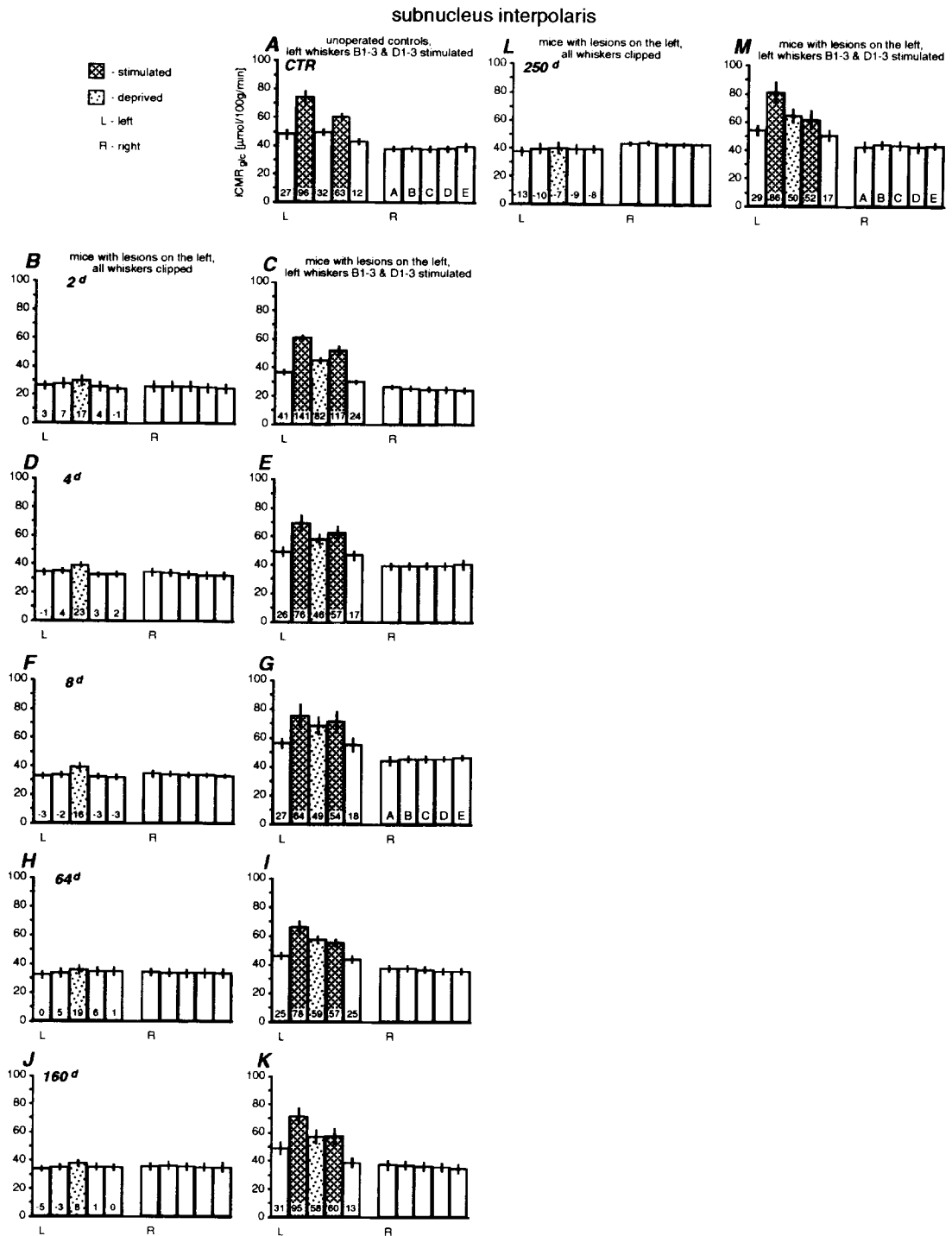


Fig. 4. Local cerebral metabolic rates for glucose ($ICMR_{glc}$) in subnucleus interpoaris. The arrangement of the bar graphs is the same as in Fig. 3. The bar graphs, labelled A–M, show the local metabolic rates ipsi- (left) and contralateral (right) to the lesion and/or stimulation. Results from stimulated unoperated mice (CTR) are shown in A. Graphs B, D, F, H, J and L show the data of mice with lesions that had all whiskers clipped before the deoxyglucose study, graphs C, E, G, I, K and M that of mice that had left whiskers B1–3 and D1–3 deflected. The lesion led to changes in $ICMR_{glc}$ similar to those in subnucleus caudalis. Metabolic rates were depressed two days after the lesion (B and C), affecting the stimulus-related response only slightly. In contrast to subnucleus caudalis however, the metabolic rate in deprived representations C1–3 was distinctly increased above control levels. Consistently, at longer time intervals after the lesion the increase in metabolic rate of the deprived territory of stimulated mice with lesions may reflect, in part, a metabolic response to the lesion itself.

that of representations D1–3. In mice with lesions, the metabolic activation of the deprived territory was greater than that of its homeotopic area in stimulated unoperated mice and in unstimulated mice with lesions at all time intervals after follicle removal. Two days after the lesion the metabolic activation of the deprived territory reached a peak in both subnuclei at on the average 2.2-times that of the homeotopic area in stimulated controls (Figs 3, 4C); it was diminished at four days (Figs 3, 4E), but rose to consolidate in both subnuclei at ~ 1.6 -times the level of stimulated controls ~ 160 days after follicle removal (Figs 3, 4K,M). The metabolic activation of the deprived territory attained the level of representations D1–3 in subnucleus interparalis (Fig. 3I,K,M) and surpassed it in subnucleus caudalis ~ 64 days after the lesion (Fig. 4I,K,M). However, it never reached the metabolic activation of representations B1–3.

Whisker stimulation resulted in the greatest percent changes in ICMR_{glc} two days after follicle removal, because it was accompanied by a general depression of ICMR_{glc} on both sides and in both unstimulated (Figs 3B, 4B) and stimulated (Figs 3C, 4C) mice. Yet whisker stimulation offset this depression and the metabolic activation of the deprived territory in subnucleus interparalis (Fig. 4C) reached statistical significance ($P \leq 0.05$; Dunnett's test). Four days after the lesion the metabolic rates had essentially returned to normal levels (Figs 3, 4D,E).

Affirming a slight metabolic response to the lesion in the deprived territory, a small, but consistent increase in ICMR_{glc} was measured in unstimulated mice with lesions. This increase was more explicit in subnucleus interparalis than in subnucleus caudalis. Its side-to-side percent difference was greatest four days after the lesion. However, even at this peak it reached only a third and a half of the metabolic activation found in the deprived territories of subnucleus caudalis and subnucleus interparalis of stimulated mice with lesions, respectively. In comparison with stimulated unoperated controls, the metabolic activity in representations C1–3 in subnucleus interparalis of stimulated mice with lesions was statistically significantly increased at all time intervals after follicle removal, except four days ($P \leq 0.05$; two-tailed Dunnett's test). Compared with unstimulated mice with lesions, this increase was statistically significant at all time intervals. The metabolic activation of the deprived territory in subnucleus caudalis did not reach statistical significance at any time interval examined. The differences in stimulus-related activation of other whisker representations were not statistically significant.

Nucleus principalis

Cytochrome oxidase activity. The whiskers on the snout are represented in the ventral aspect of nucleus principalis. As in the two subnuclei, the five rows of cytochrome oxidase-rich segments representing the

tall whiskers were distinct (Fig. 5). Eight days after follicle removal, small cavities appeared at the lateral boundary of the middle row of segments, i.e. in the territory deprived by the lesion (Fig. 5,8^d). The cavities were absent at longer time intervals after the lesion.

Metabolic activation. The stimulation of whiskers B1–3 and D1–3 increased metabolic activity in ipsilateral nucleus principalis at its lateral boundary (Fig. 5). In unoperated mice, two separate areas of high metabolic activation were distinct (Fig. 5CTR). Their location was congruent with the cytochrome oxidase-rich segments representing the stimulated whiskers. The metabolic activation of representations D1–3 was smaller than that of B1–3. Both areas stood out clearly separated from each other. In contrast, two and four days after the lesion, one large area of high metabolic activity covered the ventral aspect of the nucleus (Fig. 5,2^d, 4^d). Beginning at eight days (8^d), the activation diminished, and the two areas were discernible again at the longest time interval examined though they remained fused (Fig. 5,250^d). In unstimulated mice with lesions, metabolic activity was uniform at all time intervals after the lesion examined, except an occasional small focus of slightly elevated metabolism (Fig. 5,4^d). In the transverse plane the area occupied by the representations of the large caudal whiskers in nucleus principalis is only about one third of that in subnucleus interparalis. Because of the small dimensions of nucleus principalis, metabolic rates were not measured.

Thalamic ventrobasal complex

The ventrobasal complex appeared as an ovoid agglomeration of darkly-stained patches of high cytochrome oxidase activity (Fig. 6). In some cases, rows of segments could be discerned. However, the whisker map could not be reconstructed with certainty. In unoperated controls, the deflection of whiskers B1–3 and D1–3 resulted in two separate areas of slightly increased metabolic activity at the lateral boundary of the complex (Fig. 6CTR). In contrast, the same whisker stimulation increased metabolic activity in one broad area in mice with lesions (Fig. 6,250^d) whereas in unstimulated mice with lesions metabolic activity remained low and uniform (Fig. 6,250^d/ns).

DISCUSSION

Morphologic and metabolic whisker representation

Cytochrome oxidase activity. The segmentation of the nuclei of termination in sections stained for cytochrome oxidase activity is identical with that in sections stained for succinic dehydrogenase

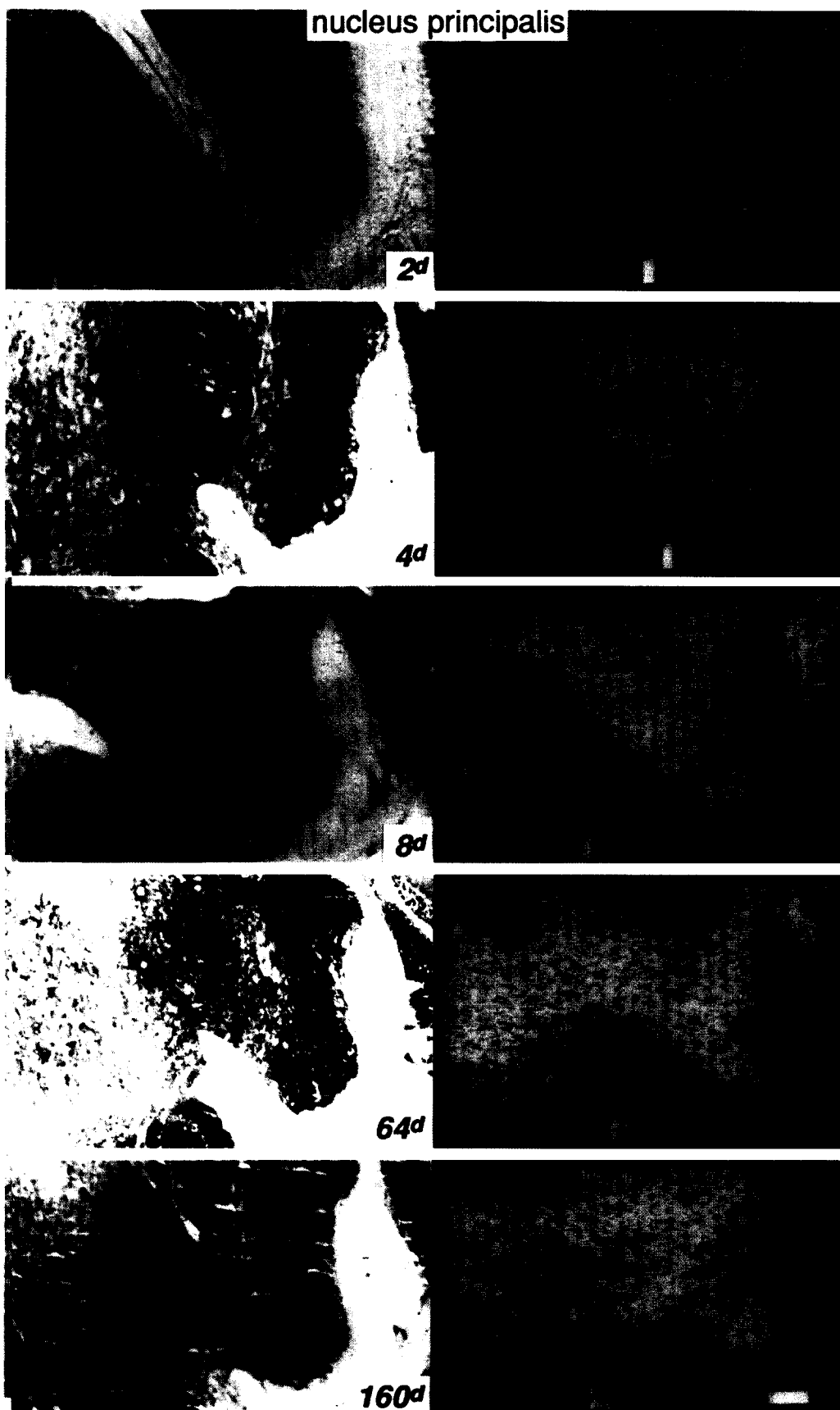


Fig. 5. (Caption on p. 56).

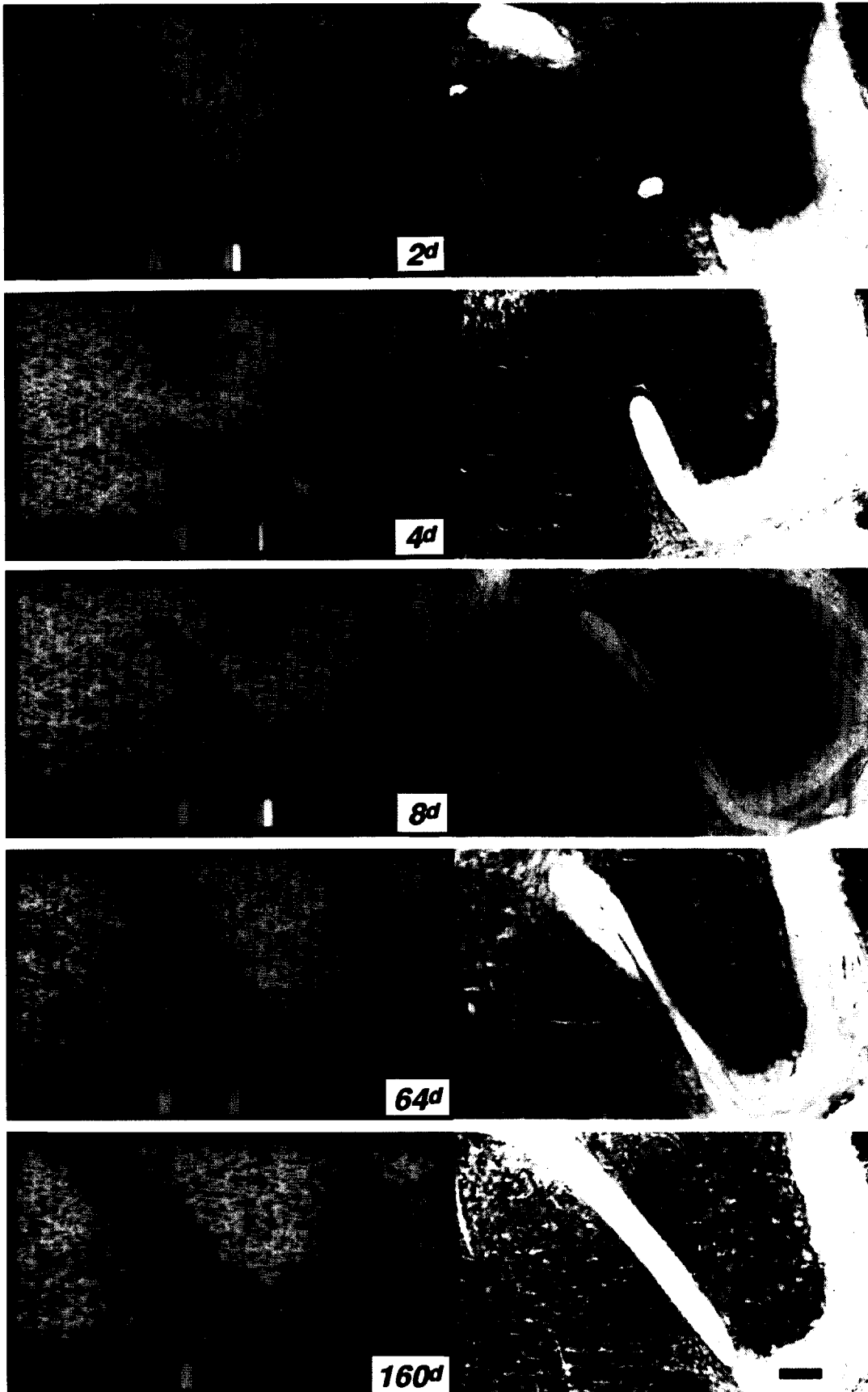


Fig. 5 (continued. Caption overleaf).

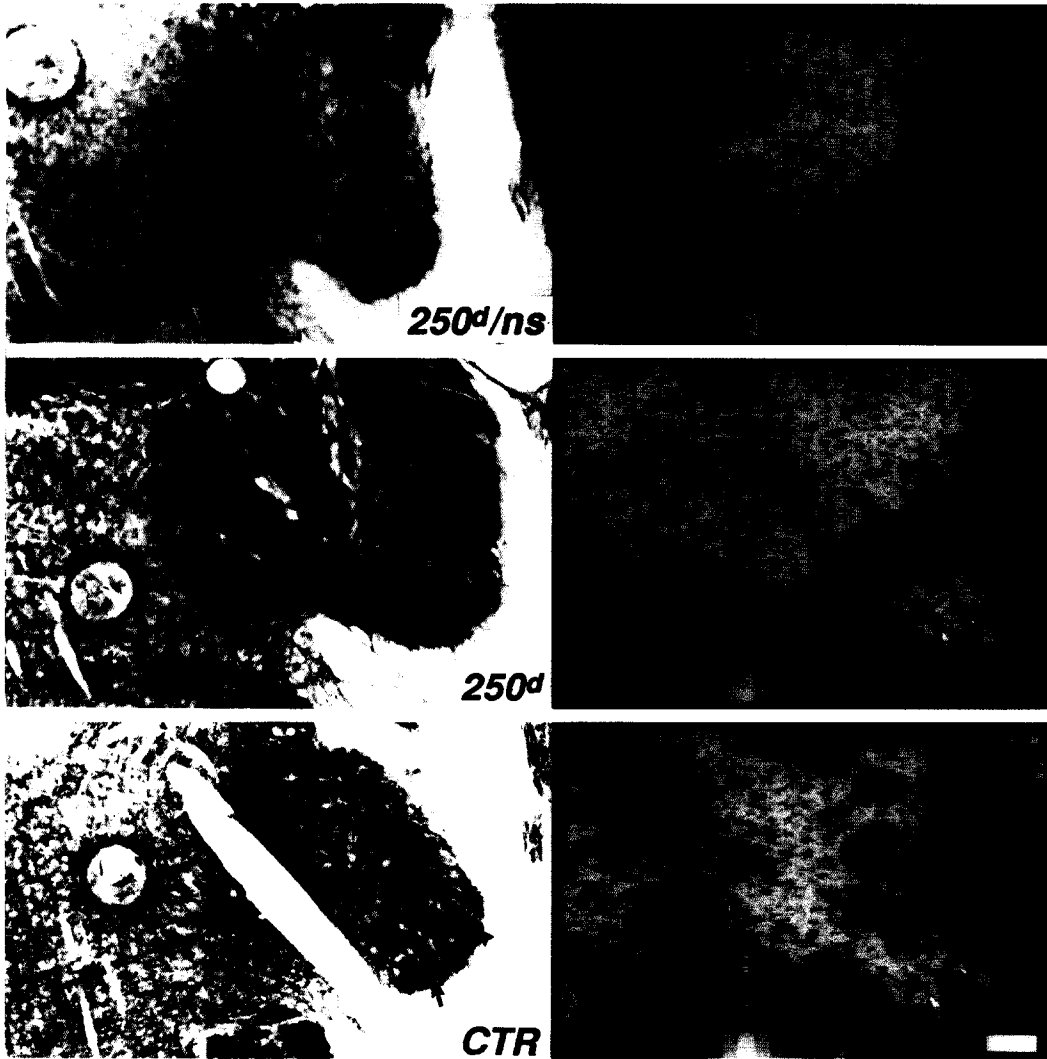


Fig. 5. Metabolic activation in nucleus principalis. The results are composed as in Fig. 1, except that only the side ipsilateral to the lesion and/or stimulation is shown. In the sections stained for cytochrome oxidase activity, the enzyme-rich segments that represent the whiskers topologically are evident. As in the two subnuclei, the five rows of segments representing the tall whiskers are distinct. In the left panel at 8^d and in CTR the arrow and the arrowhead point to the segments representing whiskers B1 and D1, respectively. Note the "cavities" lacking enzyme activity in the deprived territory between segment rows B and D eight days after the lesion (8^d). Such signs of degeneration were not found at longer time intervals after the lesion. The colour-coded images show that whisker stimulation led to one large area of increased metabolic activity (white/red is high, blue is low) at the lateral boundary of the nucleus two (2^d) and four days (4^d) after the lesion. At eight days this area was less cohesive (8^d). In unstimulated mice with lesions metabolic activation was absent, except a small focus of slightly elevated metabolism at four days (4^d; arrow). At 250 days after follicle removal, whisker stimulation resulted in a broad area of metabolic activation (250^d). However, two foci were discernible at the representations of the stimulated whiskers (250^d; arrows). In contrast, in unoperated mice these two foci were more discrete and distinctly separate (CTR; arrows). Orientation: dorsal is up, lateral is on the right; scale bars at 160^d and CTR=250 μm).

activity.^{6,12} The segments co-localize with the foci of endings of primary afferents demonstrated with horseradish peroxidase transport.^{5,34} After deafferentation cytochrome oxidase activity diminishes in postsynaptic dendrites.⁴³ Accordingly, in the present study whisker follicle removal resulted in a slight, temporary diminution of enzyme activity in the deprived segments of subnucleus caudalis two months after the lesion. No changes in enzyme

activity were detected in subnucleus interpolaris. A week after the lesion, cavities void of cytochrome oxidase activity developed temporarily in nucleus principalis. The disparate response to the lesion in the three nuclei may reflect differences in the subsets of primary afferents that each nucleus receives.⁴ The transience of the changes in subnucleus caudalis and nucleus principalis may be indicative of the restoration of active input.

ventrobasal complex

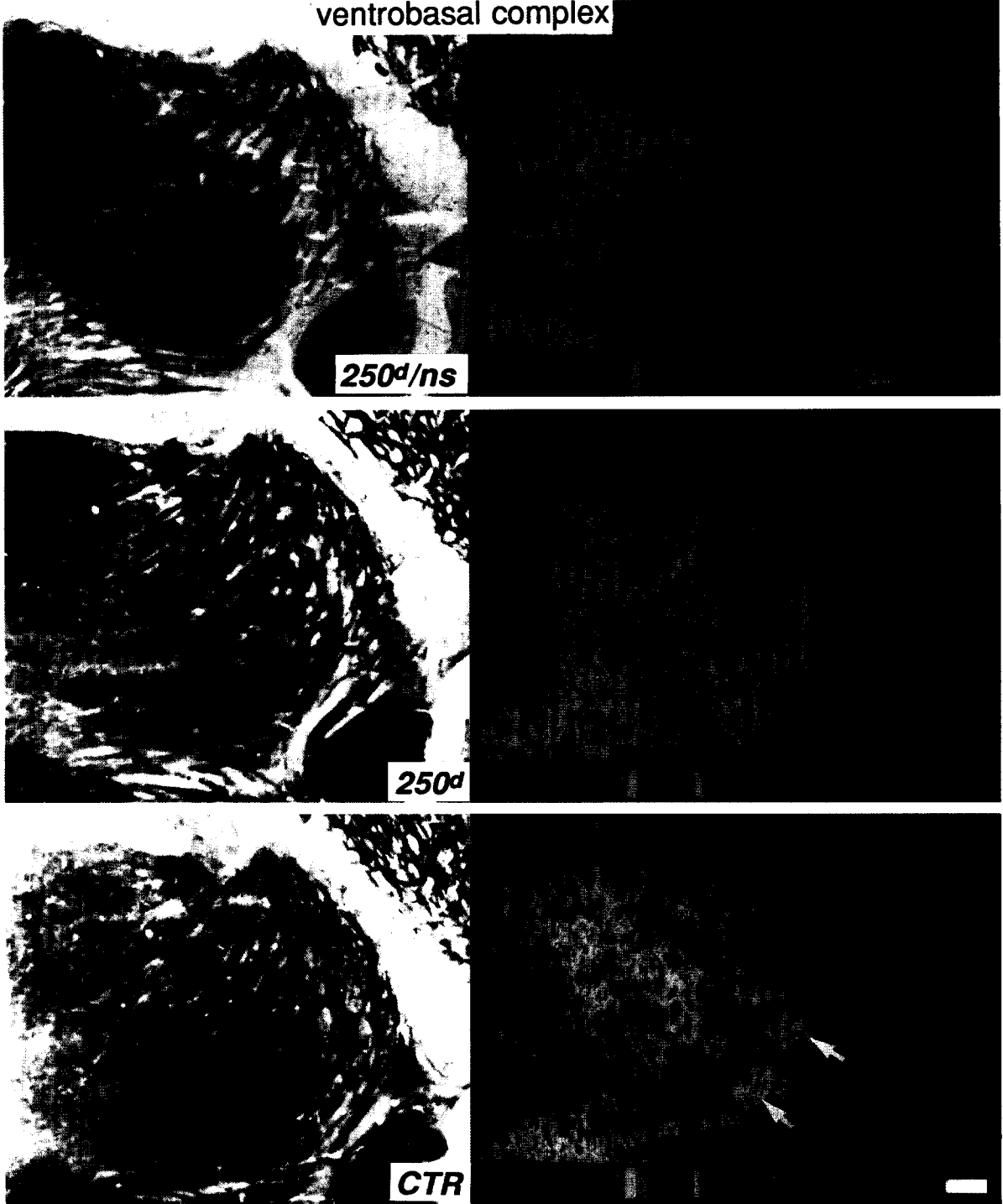


Fig. 6. Metabolic activation in the thalamic ventrobasal complex. Results obtained at the longest time interval after the removal of whisker follicles, i.e. ~ 250 days, are shown for mice with lesions that had all whiskers clipped prior to the deoxyglucose study ($250^d/n.s.$) as well as mice with lesions (250^d) and unoperated mice (CTR) that had left whiskers B1-3 and D1-3 stimulated during the deoxyglucose study. Left column: sections cut in a nearly horizontal plane and stained for cytochrome oxidase activity after autoradiography. The nucleus can be identified as an ovoid agglomeration of darkly-stained patches at the middle of the micrographs. In CTR segmentation can be discerned. However, the whisker map could not be reconstructed. Right column: colour-coded images of the autoradiograms taken from the sections. The degree of metabolic activity is expressed by the colours in the bar beneath each image (white/red is high, blue is low). Metabolic activity in unstimulated mice with lesions was low and uniform ($250^d/n.s.$) whereas stimulated mice with lesions showed increased metabolic activity in a broad area at the lateral boundary of the nucleus (250^d). In contrast, in stimulated unoperated mice two separate areas of high metabolic activity could be differentiated (CTR; arrows). The orientation of these areas agrees well with known somatotopic histochemical and cytoarchitectonic whisker maps (rostral is up, lateral is on the right; scale bar in the panel of CTR=250 μ m).

Somatotopy. Neural stimulation increases metabolic activity predominantly in the terminations of afferents,²² and the findings of the present study concur with this notion. In subnuclei caudalis and interpolaris as well as in nucleus principalis whisker row A is represented ventrally and row E dorsally. The loci of increased metabolic activity in the present study are in agreement with the finding that the primary afferents from caudal whisker follicles terminate medially in subnucleus caudalis^{1,18} and laterally in subnucleus interpolaris^{1,21} and nucleus principalis.⁵ In the latter, metabolic activation appeared less delineated than in the subnuclei. In harmony, Jacquin *et al.*,²⁰ using a high resolution deoxyglucose method, observed increased tracer accumulation in ectopic locations in this nucleus whereas the tracer accumulation in the subnuclei was restricted to the cytochrome oxidase-rich segments in which the appropriate primary afferents terminate.^{5,9,34}

In the ventrobasal complex, we could not ascertain a morphological whisker map. Ivy and Killackey¹⁵ observed that the segmentation in sections stained for succinic dehydrogenase activity disintegrates with age, and the clearest morphological maps have been demonstrated successfully in mice younger than three months.^{12,40,44} According to these maps, whisker row A is represented caudally and row E rostrally, while the caudal whiskers are represented laterally. In comparison with the prominent metabolic activation in the brainstem subnuclei, that in the ventrobasal complex appeared low and less delineated. In harmony, Jacquin *et al.*²⁰ found inconsistent deoxyglucose accumulation in the ventroposterior medial nucleus of the hamster. Apparently, the stimulation of a select few whiskers affects metabolic activity in the ventrobasal complex to only a minute degree. In spite of this complication, we could identify two areas of metabolic activation that were situated at the lateral boundary of the complex in agreement with the known somatotopy. The caudal area may represent whiskers B1–3 and the rostral area whiskers D1–3.

Plasticity

Metabolic mapping with the deoxyglucose method clearly demonstrated that the removal of three whisker follicles from adult mice leads to early prominent and persistent changes in metabolic whisker maps at the first synapse of the whisker-to-barrel pathway, i.e. the brainstem trigeminal sensory nuclei. The metabolic representations of whiskers surrounding the lesion enlarged into the deprived territory two days after follicle removal, i.e. at the shortest time interval examined, and this enlargement persisted until the end of the present investigation at approximately 10 months. At that time, the metabolic whisker maps in the thalamic ventrobasal complex and in barrel cortex²⁸ were altered in a similar

fashion, providing evidence that the modification of the whisker map eventually comprehends all relay stations of the pathway.

The removal of whisker follicles *per se* had a minor influence on the metabolic activity in the nuclei of termination. We observed only a small increase in metabolic activity in the deprived representations, greatest four and eight days after the lesion. Concomitantly, the population density of microglia increases at that location.³¹ Microglial proliferation³⁹ and phagocytosis of degenerating neurons² may increase local rates of glucose utilization. Since the resulting metabolic activity was only about half of that measured after the stimulation of whiskers adjacent to the lesion, stimulation effectively drove metabolic activity in the deprived territory. Though the increase in metabolic responsiveness of the deprived territory was immediate and persistent, the mechanisms underlying this change may vary in short- (<8 days) and long-term.

Early mechanisms. As in barrel cortex,²⁸ the local metabolic rates of all assessed areas in subnuclei caudalis and interpolaris were reduced two days after follicle removal, i.e. the earliest time interval examined. In contrast to barrel cortex however, the stimulus-related increases in metabolic activity in the representations of the stimulated whiskers were similar in mice with and without lesions. In the deprived territory metabolic activation was statistically significantly increased in subnucleus interpolaris as early as two days after the lesion. In subnucleus caudalis this metabolic activation became prominent at four days and reached a level that was on the average equal to that in subnucleus interpolaris. However, it did not reach statistical significance at any time interval examined, probably because the dimensions of the whisker representations were at the limit of the spatial resolution of the method.

Nucleus principalis is regarded as the main relay station for the ascending connections in the whisker-to-barrel pathway and appears to play a crucial role in plasticity during development.^{12,19,24} It contains 75% of the trigeminothalamic projection neurons in the murine trigeminal sensory brainstem whereas subnuclei interpolaris and caudalis accommodate only 17 and 6%, respectively.⁷ However, in spite of this imbalance, inputs to the thalamic ventrobasal complex from subnucleus interpolaris play an important role for the size of neuronal receptive fields in the thalamic relay.³⁷ Though metabolic activity was not measurable in nucleus principalis in the present study, colour-coded images showed the largest expansions of metabolic activation at two and four days, indicating an early effect of the lesion also in this nucleus.

The findings of the present study do not permit a distinction between the contributions of each brainstem nucleus to the plasticity of the higher stations. Yet, taken together they provide strong evidence for

a pronounced modification of the metabolic whisker map in the trigeminal brainstem within the first week after follicle removal. In harmony, neural receptive fields were found to be enlarged in the dorsal horn of the spinal cord four days after peripheral nerve transection.¹⁰ By contrast, primary afferents were shown to have sprouted only at one week⁴² and there is no evidence that the early modification of somatic representation at the first synapse of the somatosensory pathway is associated with new growth of connections of the primary neurons.

Two alternatives have been discussed in the literature. Devor and Wall¹⁰ suggested that the rapid enlargement of neural receptive fields was the result of changes in the efficacy of synaptic transmission caused by the removal of dominant inputs that unmask hitherto silenced inputs from soma unaffected by the lesion. Cortical synaptic strength can be shifted by *N*-methyl-D-aspartate receptor-mediated long-term potentiation and depression.²⁵ However, such mechanisms await to be demonstrated in the trigeminal brainstem.

Disinhibition is an alternative mechanism for the enlargement of neural receptive fields.⁸ Local circuit neurons that are presumably GABAergic and inhibitory have been demonstrated in subnuclei caudalis³⁵ and interpolaris.^{16,17} Their axons are recurrent and send collaterals to the other trigeminal sensory brainstem nuclei where they end in glomeruli containing synaptic triads of large symmetric, axodentritic synapses and small asymmetric, axoaxonic or axodentritic synapses.¹⁴ The removal of whisker follicles may shut down the asymmetric, putatively inhibitory, synapses and disinhibit the symmetric, putatively excitatory, synapses leading to a rapid enlargement of whisker representation.

Peculiarly, the metabolic activation of the deprived territory in the brainstem increased during a period when only a small and statistically insignificant increase in metabolic activity was detected in the deprived barrels of barrel cortex. This dissociation indicates that neural activation at the first synapse was not transmitted to the last synapse of the pathway immediately. Therefore, cortical alterations in whisker representation do not merely reflect brainstem plasticity suggesting that differing mechanisms may underlie the plasticity of various synaptic relay stations of a sensory pathway.

Late mechanisms. The large expansion of metabolic activation that was observed in nucleus principalis two and four days after follicle removal waned and was replaced by a stronger activation pattern similar to that in the subnuclei at the longest time interval examined. In conjunction with the concomitant oscillations of metabolic activation in the subnuclei, the fluctuation in nucleus principalis may constitute an actual attribute of the change in whisker representation after follicle removal. An analogous fluctuation has been demonstrated for the

sizes of neural receptive field in primary somatosensory cortex.^{8,23} However, we did not observe an early expansion of metabolic whisker representation in barrel cortex.²⁸ Since the receptive field recordings were carried out on anaesthetized animals, anaesthesia may block the neural circuitry that restricts cortical whisker representation in the awake, freely-moving mice.

Because cortical metabolic whisker representations in the animals of the present study were altered statistically significantly only after more than two months, reinnervation of the sensory periphery by regenerated nerve fibres^{28,32} may exert a crucial influence on central whisker representations. Skin denervated by crush or transection of the sciatic nerve in adult rats may be reinnervated by either sprouting saphenic or regenerating sciatic nerve fibres.¹¹ Consistent with such flexibility, infraorbital nerve transection results in the loss of somatotopy of Gasserian ganglion cells³⁶ and terminations of primary afferents.^{3,33} Moreover, after follicle removal follicles of adjacent whiskers receive novel innervation,²⁸ and this reorganization of peripheral innervation may be sufficient to explain the observed changes in central somatotopy.

However, the endings of primary afferents may also reorganize. In macaques the transection of the median nerve led to the expansion of its central terminations in the dorsal horn of the spinal cord and in the cuneate nucleus, and this expansion was reflected in a changed organization of receptive fields in primary somatosensory cortex.¹³ In accord, after infraorbital nerve transection in adult rats neural receptive fields in the nuclei of termination were expanded and, on occasion, divided.²⁶ Therefore, whether the endings of primary afferents expand under the conditions of the present study is an interesting question to be addressed in the future.

Comparison with developmental plasticity. In a previous study we removed whisker follicles C1–3 from neonates and in their adulthood subjected them to whisker stimulation while ICMR_{glc} was measured with the [¹⁴C]2-deoxyglucose method.²⁹

Cytochrome oxidase activity in the deprived territory of the three brainstem nuclei was distinctly diminished and in nucleus principalis adjacent segments were enlarged. As in the present study, the deprived territory was metabolically activated by the stimulation of whiskers adjacent to the lesion. Whereas in subnucleus caudalis this activation was about the same as that at the longest time interval in the present study, it was only half of that in subnucleus interpolaris. This discrepancy points to a difference in vulnerability of primary afferents to whisker follicle removal during development.

In the thalamic ventrobasal complex, whisker follicle removal in neonates resulted in the loss of differentiable metabolic activation whereas removal of the same follicles in adults led to a metabolic

activation pattern similar to that in the brainstem. This discrepancy may be the result of a difference in the capacity of axotomized primary neurons to recuperate. Regenerating nerve fibres were not seen in the whiskerpads of the mice with neonatal lesions, and ganglion cells were likely to die.⁴¹ The ensuing atrophy of the deprived morphological representations in the nuclei of termination suggests that brainstem projection neurons degenerated after the deafferentation. Consistently, a similar atrophy of the deprived territory has been observed in the ventrobasal complex.^{6,12} Therefore, after neonatal whisker follicle removal the remaining input to the ventrobasal complex from the deprived territories in the brainstem must be small. In contrast, after whisker follicle removal in adults axotomized nerve fibres regenerate vigorously and reinnervate the sensory periphery. Atrophy of the deprived territories in the brainstem is slight and transient. Thus, a strong connection with the ventrobasal complex may remain. This connection may be crucial for the maintenance of the metabolic activation found in the present study. Moreover, it may stabilize the morphological whisker map in barrel cortex which, unlike in mice with neonatal lesions, did not change.²⁸

CONCLUSION

The present report and its preceding companion demonstrate that the removal of three whisker follicles in adult mice results in the enlargements of the

functional representations of intact whiskers adjacent to the lesion into the deprived territory in the whisker-to-barrel pathway. This plasticity has two compelling aspects: i) the whisker map in the nuclei of termination is modified early without affecting barrel cortex, and ii) a similar, late modification evolves in barrel cortex gradually and concomitantly with the reinnervation of the periphery. Whereas the early modification of the whisker map in the brainstem may be explained with unmasking of hitherto suppressed inputs, the late modifications are most likely the result of altered peripheral sensory innervation and/or altered primary afferents. The delayed evolution of a new responsiveness in barrel cortex may provide an opportunity for a novel innervation of the sensory periphery to influence cortical plasticity. The present investigation covered a good third of the mature life of the albino mouse, and apparently regenerated peripheral nerve fibres continued to find and innervate whisker follicles up to the very end.²⁸ Hence, facilitation of the reinnervation of the sensory periphery even at a long time interval after the lesion may possibly exert a beneficial influence on the recovery of function, and this potential will be subject of future investigations.

Acknowledgements—We are indebted to L. Sokoloff for many helpful comments and his unrelenting support. J. D. Brown, J. Jehle, J. Kang, E. Lewis, K. Schmidt and Y. L. Sun were of invaluable help during various phases of the study.

REFERENCES

1. Arvidsson J. (1982) Somatotopic organization of vibrissae afferents in the trigeminal sensory nuclei of the rat studied by transganglionic transport of HRP. *J. comp. Neurol.* **211**, 84–92.
2. Arvidsson J. (1986) Transganglionic degeneration in vibrissae innervating primary sensory neurons of the rat: A light and electron microscopic study. *J. comp. Neurol.* **249**, 392–403.
3. Arvidsson J. and Johansson K. (1988) Changes in the central projection pattern of vibrissae innervating primary sensory neurons after peripheral nerve injury in the rat. *Neurosci. Lett.* **84**, 120–124.
4. Arvidsson J. and Rice F. L. (1991) Central projections of primary sensory neurons innervating different parts of the vibrissae follicles and intervibrissal skin on the mystacial pad of the rat. *J. comp. Neurol.* **309**, 1–16.
5. Bates C. A. and Killackey H. P. (1985) The organization of the neonatal rat's brainstem trigeminal complex and its role in the formation of central trigeminal patterns. *J. comp. Neurol.* **240**, 265–287.
6. Belford G. R. and Killackey H. P. (1979) Vibrissae representation in subcortical trigeminal centers of the neonatal rat. *J. comp. Neurol.* **183**, 305–322.
7. Bruce L. L., McHaffie J. G. and Stein B. E. (1987) The organization of trigeminothalamic and trigeminothalamic neurons in rodents: A double-labeling study with fluorescent dyes. *J. comp. Neurol.* **262**, 315–330.
8. Calford M. B. and Tweedale R. (1988) Immediate and chronic changes in responses of somatosensory cortex in adult flying-fox after digit amputation. *Nature* **332**, 446–448.
9. Chiaia N. L., Bennett-Clarke C. A., Eck M., White F. A., Crissman R. S. and Rhoades R. W. (1992) Evidence for prenatal competition among the central arbors of trigeminal primary afferent neurons. *J. Neurosci.* **12**, 62–76.
10. Devor M. and Wall P. D. (1981) Plasticity in the spinal cord sensory map following peripheral nerve injury in rats. *J. Neurosci.* **1**, 679–684.
11. Devor M., Schonfeld D., Seltzer Z. and Wall P. D. (1979) Two modes of cutaneous reinnervation following peripheral nerve injury. *J. comp. Neurol.* **185**, 211–220.
12. Durham D. and Woolsey T. A. (1984) Effects of neonatal whisker lesions on mouse central trigeminal pathway. *J. comp. Neurol.* **223**, 424–447.
13. Florence S. L., Garraghty P. E., Wall J. T. and Kaas J. H. (1994) Sensory afferent projections and area 3b somatotopy following median nerve cut and repair in macaque monkeys. *Cerebr. Cortex* **4**, 391–407.
14. Ide L. S. and Killackey H. P. (1985) Fine structural survey of the rat's brainstem sensory trigeminal complex. *J. comp. Neurol.* **235**, 145–168.
15. Ivy G. O. and Killackey H. P. (1982) Ephemeral cellular segmentation in the thalamus of the neonatal rat. *Devl Brain Res.* **2**, 1–17.
16. Jacquin M. F., Golden J. and Rhoades R. W. (1989) Structure–function relationships in rat brainstem subnucleus interpolaris. III. Local circuit neurons. *J. comp. Neurol.* **282**, 24–44.

17. Jacquin M. F., Barcia M. and Rhoades R. W. (1989) Structure–function relationships in rat brainstem subnucleus interpolaris. IV. Projection neurons. *J. comp. Neurol.* **282**, 45–62.
18. Jacquin M. F., Renehan W. E., Mooney R. D. and Rhoades R. W. (1986) Structure–function relationships in rat medullary and cervical dorsal horns. I. Trigeminal primary afferents. *J. Neurophysiol.* **55**, 1153–1186.
19. Jacquin M. F., Rana J. Z., Miller M. W., Chiaia N. L. and Rhoades R. W. (1996) Development of trigeminal nucleus principalis in the rat – effects of target removal at birth. *Eur. J. Neurosci.* **8**, 1641–1657.
20. Jacquin M. F., McCasland J. S., Henderson T. A., Rhoades R. W. and Woolsey T. A. (1993) 2-DG uptake patterns related to single vibrissae during exploratory behaviors in the hamster trigeminal system. *J. comp. Neurol.* **332**, 38–58.
21. Jacquin M. F., Woerner D., Szczepanik A. M., Riecker V., Mooney R. D. and Rhoades R. W. (1986) Structure–function relationships in rat brainstem subnucleus interpolaris. I. Vibrissa primary afferents. *J. comp. Neurol.* **243**, 266–279.
22. Kadekaro M., Crane A. M. and Sokoloff L. (1985) Differential effects of electrical stimulation of sciatic nerve on metabolic activity in spinal cord and dorsal root ganglion in the rat. *Proc. natn. Acad. Sci. U.S.A.* **82**, 6010–6013.
23. Kelahan A. M. and Doetsch G. S. (1984) Time-dependent changes in the functional organization of somatosensory cerebral cortex following neonatal digit amputation in adult raccoons. *Somatosensory Res.* **2**, 49–81.
24. Killackey H. P. and Fleming K. (1985) The role of the principal sensory nucleus in central trigeminal pattern formation. *Devl Brain Res.* **22**, 141–145.
25. Kirkwood A., Rioult M. and Bear M. F. (1996) Experience-dependent modification of synaptic plasticity in visual cortex. *Nature* **381**, 526–528.
26. Klein B. G. (1991) Chronic functional consequences of adult infraorbital nerve transection for rat trigeminal subnucleus interpolaris. *Somatosensory Res.* **8**, 175–191.
27. Ma P. and Woolsey T. A. (1984) Cytoarchitectonic correlates of the vibrissae in the medullary trigeminal complex of the mouse. *Brain Res.* **306**, 374–379.
28. Melzer P. and Smith C. B. Plasticity of cerebral metabolic whisker maps in adult mice after whisker follicle removal: I) Modifications in barrel cortex coincide with reorganization of follicular innervation. *Neuroscience*. (submitted for publication).
29. Melzer P. and Smith C. B. (1996) Plasticity of metabolic whisker maps in somatosensory brainstem and thalamus of mice with neonatal lesions of whisker follicles. *Eur. J. Neurosci.* **8**, 1853–1864.
30. Melzer P. and Smith C. B. (1995) Plasticity of the metabolic whisker map in the mouse somatosensory system after follicle removal in neonates and in adults. *J. cerebr. Blood Flow Metab.* **15 Suppl. 1**, S685.
31. Melzer P., Zhang M.-Z. and McKanna J. A. (1997) Infraorbital nerve transection and whisker follicle removal in adult rats affect microglia and astrocytes in the trigeminal brainstem. A study with Lipocortin1- and S100 β -immunohistochemistry. *Neuroscience*, **80**, 459–472.
32. Renehan W. E. and Munger B. L. (1986) Degeneration and regeneration of peripheral nerve in the rat trigeminal system. II. Response to nerve lesions. *J. comp. Neurol.* **249**, 429–459.
33. Renehan W. E., Rhoades R. W. and Jacquin M. F. (1989) Structure–function relationships in rat brainstem subnucleus interpolaris: VII. Primary afferent central terminal arbors in adults subjected to infraorbital nerve section at birth. *J. comp. Neurol.* **289**, 493–508.
34. Renehan W. E., Crissman R. S. and Jacquin M. F. (1994) Primary afferent plasticity following partial denervation of the trigeminal brainstem nuclear complex in the postnatal rat. *J. Neurosci.* **14**, 721–739.
35. Renehan W. E., Jacquin M. F., Mooney R. D. and Rhoades R. W. (1986) Structure–function relationships in rat medullary and cervical dorsal horns. II. Medullary dorsal horn cells. *J. Neurophysiol.* **55**, 1187–1201.
36. Renehan W. E., Chiaia N. L., Klein B. G., Jacquin M. F. and Rhoades R. W. (1989) Physiological and anatomical consequences of infraorbital nerve transection in the trigeminal ganglion and trigeminal spinal tract of the adult rat. *J. Neurosci.* **9**, 548–557.
37. Rhoades R. W., Belford G. R. and Killackey H. P. (1987) Receptive-field properties of rat ventral posterior medial neurons before and after selective kainic acid lesions of the trigeminal brain stem complex. *J. Neurophysiol.* **57**, 1577–1600.
38. Sokoloff L., Reivich M., Kennedy C., Des Rosier D. H., Patlak C. S., Pettigrew K. D., Sakurada O. and Shinohara M. (1977) The [¹⁴C]deoxyglucose method for the measurement of local cerebral glucose utilization: Theory, procedure and normal values in the conscious and anesthetized albino rat. *J. Neurochem.* **28**, 897–916.
39. Streit W. J. and Kreutzberg G. W. (1988) Response of endogenous glial cells to motor neuron degeneration induced by toxic ricin. *J. comp. Neurol.* **268**, 248–263.
40. Van der Loos H. (1976) Barreloids in mouse somatosensory thalamus. *Neurosci. Lett.* **2**, 1–6.
41. Waite P. M. E. (1984) Rearrangement of neuronal responses in the trigeminal system of the rat following peripheral nerve section. *J. Physiol., Lond.* **352**, 425–445.
42. Woolf C. J., Shortland P. and Coggeshall R. E. (1992) Peripheral nerve injury triggers central sprouting of myelinated afferents. *Nature* **355**, 75–78.
43. Wong-Riley M. T. T. (1989) Cytochrome oxidase: An endogenous metabolic marker for neuronal activity. *Trends Neurosci.* **12**, 94–101.
44. Yamakado M. (1985) Postnatal development of barreloid neuropils in the ventrobasal complex of mouse thalamus: A histochemical study for cytochrome oxidase. *Brain and Nerve* **37**, 497–506.

(Accepted 16 June 1997)